

# Parameterising the third dredge-up in asymptotic giant branch stars

A. I. Karakas,<sup>1</sup> J. C. Lattanzio,<sup>1</sup> & O. R. Pols<sup>2,1</sup>

<sup>1</sup> School of Mathematical Sciences, Monash University, Wellington Rd, Clayton, Australia, 3800  
amanda.karakas@maths.monash.edu.au

<sup>2</sup> Astronomical Institute Utrecht, Postbus 80000, 3508 TA Utrecht, the Netherlands

## Abstract

We present new evolutionary sequences for low and intermediate mass stars ( $1M_{\odot}$  to  $6M_{\odot}$ ) for three different metallicities,  $Z = 0.02; 0.008$  and  $0.004$ . We evolve the models from the pre-main sequence to the thermally-pulsing asymptotic giant branch phase. We have two sequences of models for each mass, one which includes mass loss and one without mass loss. Typically 20 or more pulses have been followed for each model, allowing us to calculate the third dredge-up parameter for each case. Using the results from this large and homogeneous set of models, we present an approximate fit for the core mass at the first thermal pulse,  $M_c^1$ , as well as for the third dredge-up efficiency parameter,  $\eta$ , and the core mass at the first dredge-up episode,  $M_c^{\text{in}}$ , as a function of metallicity and total mass. We also examine the effect of a reduced envelope mass on the value of  $\eta$ .

**Key words:** stars: AGB and post-AGB { stars: evolution { stars: interiors { stars: low mass

## 1 Introduction

The ascent of the asymptotic giant branch (AGB) is the final nuclear-burning stage in the life of stars with masses between about 1 and  $8M_{\odot}$ . The combination of extensive nucleosynthesis and high mass loss makes these stars crucial for understanding the chemical composition of galaxies. For recent reviews see Iben (1991), Frost & Lattanzio (1995) and Busso, Gallino & Wasserburg (1999).

Very briefly, an AGB star is characterized by two nuclear burning shells, one burning helium (He) above a degenerate carbon-oxygen core and another burning hydrogen (H), below a deep convective envelope as shown in Figure 1. The He-burning shell is

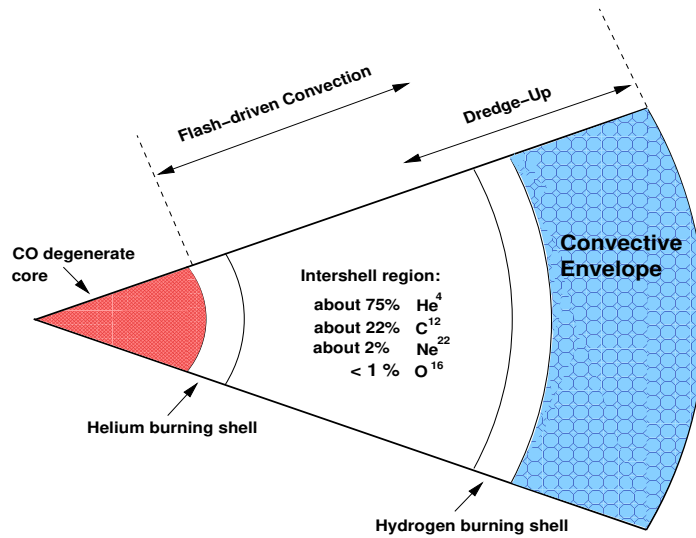


Figure 1: Schematic structure of an AGB star, showing the degenerate CO core surrounded by a He-burning shell above the core and a H-burning shell below the deep convective envelope. The burning shells are separated by an intershell region rich in helium ( 75% ) and carbon ( 22% ) with some oxygen. Note this diagram is not to scale. The ratio of the radial thickness of the H-exhausted core compared to the envelope is about  $1 \cdot 10^{-5}$ .

They are thermally unstable, and pulse every  $10^4$  years or so, depending on the core mass<sup>1</sup> and composition of the star. In each thermal pulse (TP), the He-burning luminosity can reach up to  $L_{\text{He}} \approx 10^8 L_{\odot}$ , most of which goes into expanding the outer layers. This strong expansion drives the H-shell to cooler, less dense regions which has the effect of extinguishing the H-shell. The inner edge of the deep convective envelope can then move inward (in mass) and mix to the surface the products of internal nucleosynthesis. This mixing event, which can occur periodically (after each TP), is known as the third dredge-up (TDU) and is the mechanism for producing (single) carbon stars. Following dredge-up, the star contracts, re-igniting the H-shell and enters a phase of quiescent H-burning, known as the interpulse phase. The thermally pulsing AGB (TP-AGB) is defined as the phase after the first thermal pulse to the time when the star ejects its envelope, terminating the AGB phase.

The efficiency of the TDU is quantified by the parameter  $\beta$ , which is the ratio of mass dredged up by the convective envelope,  $M_{\text{dredge}}$ , to the amount by which the core mass increased due to H-burning during the preceding interpulse period,  $M_{\text{c}}$ ,

$$\beta = \frac{M_{\text{dredge}}}{M_{\text{c}}} \quad (1)$$

The value of  $\beta$  depends on physical parameters such as the core mass, metallicity (and hence opacity) as well as the total mass of the star. Exactly how  $\beta$  depends on

<sup>1</sup>unless otherwise specified, by "core" we mean the H-exhausted core

these quantities is still unknown. The two main reasons for this are the difficulty in locating the inner edge of the convective envelope during the dredge-up phase (Frost & Lattanzio 1996, Mowlavi 1999) and the huge computer resources required to explore an appropriate range of mass and composition over such a computationally demanding evolutionary phase. Without a systematic investigation of the dredge-up law, only certain trends have been identified by extant models, such as the increase of  $\tau$  with decreasing  $Z$  and increasing mass (Boothroyd & Sackmann 1988), and the fact that below some critical envelope mass, the dredge-up ceases altogether (Straniero et al. 1997).

The convenient fact that the stellar luminosity on the AGB is a nearly linear function of the H-exhausted core mass has stimulated the development of "synthetic" AGB evolution models, as a quick way of simulating stellar populations on the AGB. The main observational constraint which models must face is the carbon star luminosity function (CSLF) for the Magellanic Clouds. In some synthetic AGB evolution calculations, e.g. as performed by Groenewegen & de Jong (1993) and Marigo (1996),  $\tau$  is treated as a constant free parameter, calibrated by comparison with the CSLF.

Synthetic codes enable us to investigate a diverse range of problems, such as binary population synthesis (Hurley, Tout & Pols, 2002), AGB population studies (Groenewegen & de Jong 1993), and the calculation of stellar yields from AGB stars (Marigo 1996, 1998a,b, 2001; van den Hoek & Groenewegen 1997). Most parameterisations used in synthetic evolution studies are found either empirically from observations (such as mass loss) or from results from full stellar calculations, such as the core-mass-interpulse-period relation. Currently there are no parameterisations in the literature based on detailed evolutionary models that describes the behaviour of  $\tau$  with total mass, metallicity, age and/or core mass, for the reasons given above.

With current computing power the problem becomes time consuming rather than impossible. Hence we have embarked on just such an exploration of relevant parameter space using full detailed evolutionary models. Our aim is to determine the dependence of evolutionary behaviour (such as the dredge-up law) on the various stellar parameters, and to provide these in a form suitable for use in synthetic population studies.

This paper is organised as follows. First we discuss the stellar evolution models and the code used to calculate them. In the second section we discuss our method for parameterising dredge-up and give the fitting formulae we found from the stellar models to describe the core mass at the first thermal pulse,  $M_c^1$ , the core mass at the first TDU episode,  $M_c^{\text{in}}$ , and  $\tau$  as functions of initial mass and metallicity. We finish with a discussion.

## 2 Stellar Models

Evolutionary calculations were performed with the Monash version of the M t Strom lo Stellar Evolution Code (Frost, 1997; Wood & Zarro, 1981) updated to include the OPA L opacity tables of Iglesias & Rogers (1996). We ran about 60 sequences of stellar models, from the zero-age main-sequence (ZAMS) to near the end of the TP-AGB for three different compositions:  $Z = 0.02; 0.008$  and  $0.004$ . For each composition we

cover a range in mass between 1 and  $6M_{\odot}$ . We do not include overshooting in the convective cores of intermediate mass stars during H burning on the main-sequence, although there is observational evidence for a small overshoot region.

## 2.1 Convection and Dredge-up

The amount of third dredge-up found in evolutionary calculations crucially depends on the numerical treatment of convective boundaries: many codes do not find any dredge-up for low mass stars without some form of overshoot (Mowlavi 1999; Herwig 1997). Herwig (2000) found very efficient dredge-up, with  $\alpha > 1$ , in a  $3M_{\odot}$   $Z = 0.02$  model with diffusive convective overshoot on all convective boundaries but no dredge-up for the same mass without overshoot. Pols & Tout (2001) found very efficient dredge-up, with  $\alpha \approx 1$ , in a  $5M_{\odot}$   $Z = 0.02$  model using a completely implicit and simultaneous solution for stellar structure, nuclear burning and convective mixing. Frost & Lattanzio (1996) found the treatment of entropy to affect the efficiency of dredge-up and Straniero et al. (1997) found the space and time resolution to be important.

In view of this strong dependence on numerical details, it is important to specify carefully how we treat convection. We use the standard mixing-length theory for convective regions, with a mixing-length parameter  $\alpha = l/H_p = 1.75$ , and determine the border by applying the Schwarzschild criterion. Hence we do not include convective overshoot, in the usual sense. We do, however, recognize the discontinuity in the ratio  $r$  of the radiative to adiabatic temperature gradients at the bottom edge of the convective envelope during the dredge-up phase. We search for a neutral border to the convective zone, in the manner described in Frost & Lattanzio (1996). Briefly, we extrapolate (linearly, in mass) the ratio  $r$  from the last convective point to the first radiative point, and if  $r > 1$  then we include this point in the convective region for the next iteration on the structure. We remind the reader that this algorithm sometimes fails, in the sense that the convective envelope grows deeper and then retreats, with succeeding iterations. In such a case, we take the deepest extent as the mixed region, even if the convective region is shallower when the model converges.

Finally we note that, although we believe our treatment of convection is reasonable, our results cannot be regarded as the definitive solution to the difficult problem of third dredge-up. However, the important point is that all our models are computed using the same algorithm. Together they constitute, for the first time, an internally consistent set of models covering a wide range in mass and metallicity.

## 2.2 Mass Loss

Mass loss is a crucial part of AGB evolution, and seriously affects dredge-up in two ways. Firstly, for the more massive stars dredge-up can be terminated when the envelope mass decreases below some critical value. Secondly, for lower masses, mass loss may terminate the AGB evolution before the H-exhausted core reaches the minimum value for dredge-up to occur. However, the mass-loss rate in AGB stars is very uncertain, and for this reason we calculate each stellar sequence both with and without

mass loss. By neglecting mass loss, we find the limiting behaviour of dredge-up for each model we calculate. In Section 3 we parameterise this dredge-up behaviour in the absence of mass loss. When this parameterisation is used in synthetic evolutionary calculations, the chosen mass-loss law will determine if the models reach the limiting behaviour we provide. The subsequent AGB evolution and dredge-up will then be modified by the choice of mass-loss law. For example, we will determine a minimum core mass for dredge-up at a given mass and composition in the case without mass loss, and whether the model reaches this core mass or not will depend on the chosen mass-loss rate. Alternatively, a particular mass-loss law may or may not prevent a model from reaching the asymptotic value for  $\dot{M}$ , which can only be determined from full stellar models without the inclusion of mass loss.

We also ran one set of models with our preferred mass-loss law. We use the Reimers (1975) formula on the red giant branch with  $\beta = 0.4$  and then the prescription of Vassiliadis & Wood (1993) (hereafter VW 93) on the AGB. VW 93 parameterised the mass-loss rate as a function of pulsation period,

$$\log \frac{dM}{dt} = 11.4 + 0.0125P; \quad (2)$$

where the mass-loss rate is in  $M_{\odot} \text{ yr}^{-1}$  and  $P$  is the pulsation period in days, given by

$$\log P = 2.07 + 1.94 \log R - 0.9 \log M; \quad (3)$$

where  $R$  and  $M$  are the stellar radius and mass in solar units. For  $P > 500$  days, the mass-loss rate given in Equation 2 is truncated at

$$\frac{dM}{dt} = \frac{L}{c v_{\text{exp}}}; \quad (4)$$

corresponding to a radiation-pressure driven wind ( $L$  is the stellar luminosity in solar units). The wind expansion velocity,  $v_{\text{exp}}$  is also taken from VW 93 and is given by

$$v_{\text{exp}} = 13.5 + 0.056P; \quad (5)$$

where  $v_{\text{exp}}$  is in  $\text{km s}^{-1}$ , and is limited to a maximum of  $15 \text{ km s}^{-1}$ .

### 2.3 Evolutionary Sequences

The models were evolved from the main-sequence, through all intermediate stages, including the core-helium flash for initial mass  $M_0 \approx 2.5 M_{\odot}$ . Most models without mass loss were evolved until  $\dot{M}$  reached an asymptotic value. Models with mass loss were evolved until convergence difficulties ceased the calculation, which was very near the end of the AGB phase. Typically the final envelope mass was quite small,  $M_{\text{env}} \approx 0.1$ , for low-mass models ( $M_0 \approx 2.5$ ) and  $M_{\text{env}} \approx 1 M_{\odot}$  for intermediate mass stars ( $M_0 \approx 3$ ). The remaining evolution is extremely brief, because the mass-loss rate is so high (typically a few times  $10^{-5} M_{\odot} \text{ yr}^{-1}$ ) at this stage.

Table 1: Initial compositions (in mass-fractions) used for stellar models:

	Z = 0.02	Z = 0.008	Z = 0.004
	solar	LM C	SM C
X	0.6872	0.7369	0.7484
Y	0.2928	0.2551	0.2476
$^{12}\text{C}$	2.9259 (-3)	9.6959 (-4)	4.8229 (-4)
$^{14}\text{N}$	8.9786 (-4)	1.4240 (-4)	4.4695 (-5)
$^{16}\text{O}$	8.1508 (-3)	2.6395 (-3)	1.2830 (-3)
Other Z	8.0253 (-3)	4.2484 (-3)	2.1899 (-3)

Evolutionary sequences were calculated for stars with masses<sup>2</sup> 1, 1.25, 1.5, 1.75, 1.9, 2, 2.1, 2.25, 2.5, 3, 3.5, 4, 5 and 6M<sub>⊙</sub>. The initial compositions used are shown in Table 1 and are similar to solar composition, Large Magellanic Cloud (LMC) and Small Magellanic Cloud (SMC) composition and were chosen to be consistent with the models of Frost (1997).

## 2.4 Model Results

We found that the third dredge-up behaviour of models that experienced the second dredge-up (SDU) (generally masses  $M_0 \lesssim 4$  depending on Z, or core masses greater than  $0.8M_{\odot}$ ), differs qualitatively from that of lower-mass models. To find them in minimum mass for the SDU for the three different compositions we ran a few models to the start of the TP-AGB only. We found the SDU at  $M > 4.05M_{\odot}$  for  $Z = 0.02$ ,  $M > 3.8M_{\odot}$  for  $Z = 0.008$  and  $M > 3.5M_{\odot}$  for  $Z = 0.004$ .

As an example of our results for higher masses, we show the  $5M_{\odot}$ ,  $Z = 0.004$  model with mass loss in Figure 2. This sequence shows 74 TPs with the last calculated model having  $M_{\text{env}} = 0.944$  and a core mass of  $M_c = 0.906$ . The dredge-up parameter is seen to increase very quickly, reaching a value near 0.96 in only four pulses and maintaining that value until the end of the calculation. We see that  $\alpha$  oscillates a little near the end, between 0.85 and 0.96; this may indicate the imprecision of the dredge-up algorithm. We find that in all our higher-mass models  $\alpha$  reached an asymptotic value of about 0.9 or higher, regardless of composition and mass loss.

Moving to the lower mass models, we first compare those with and without mass loss. Models with mass loss have shallower dredge-up, sometimes none at all, compared to the limiting values found with constant mass. We note that many of the models with mass loss do not reach the minimum core mass for TDU,  $M_c^{\text{min}}$ . We will therefore parameterize  $M_c^{\text{min}}$  from models without mass loss.

As with previous calculations (Boothroyd & Sackmann 1988; Vassiliadis 1992; Straniero 1997) we found that  $\alpha$  increases with decreasing metallicity for a given mass (with or without mass loss) for the lower-mass models. For example we found no dredge-up for a  $1.75M_{\odot}$ ;  $Z = 0.02$  model with mass loss but the  $1.75M_{\odot}$ ;  $Z = 0.004$

<sup>2</sup>Note all masses quoted are the ZAMS initial mass, in solar units, unless otherwise stated.

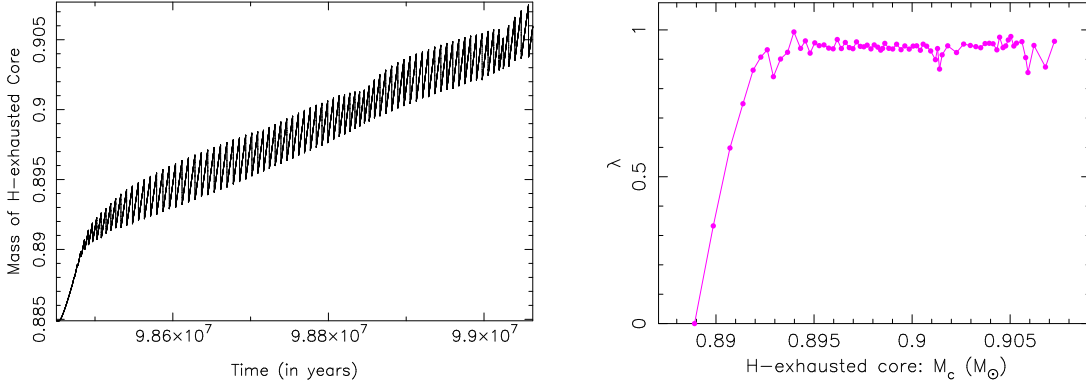


Figure 2: (Left) H-exhausted core mass  $M_c$  against time (years) for the  $5M_{\odot}$ ,  $Z = 0.004$  model with mass loss. This calculation covered 74 pulses, which equated to roughly  $7 \times 10^5$  individual stellar models. (Right) The dredge-up parameter  $\lambda$  against core mass. Dredge-up increased very quickly with pulse number, reaching 0.9 within four TPs.

model with mass loss became a carbon star, with a maximum  $\lambda = 0.6$ , as shown in Figure 3.

One of the aims of the models with mass loss was to examine how  $\lambda$  decreases with decreasing envelope mass,  $M_{\text{env}}$ , and the critical envelope mass for which dredge-up ceases. Unfortunately, the higher mass models ( $M = 6$  & 3) suffered convergence problems before reaching this critical envelope mass. We find no systematic decrease of  $\lambda$  as the envelope mass decreases (see Fig. 2). For  $Z = 0.004$  and  $Z = 0.008$ , the low-mass models that do experience dredge-up have  $\lambda > 0$  as long as  $M_{\text{env}} \approx 0.2$ , which is thus our estimate of the critical envelope mass for TDU to occur.

Table 2 presents results for the  $Z = 0.02$  models with ( $M = 6$ ) and without mass loss ( $M = 0$ ). The first column shows the initial mass ( $M_0$ ), and the zero-age horizontal branch (ZAHB) mass in parentheses for low-mass stars. The second column gives the core mass at the first thermal pulse,  $M_c^1$ , column three gives  $\lambda_{\text{max}}$ , the maximum  $\lambda$  for that model, column four the core mass at the first dredge-up episode,  $M_c^{\text{in}}$  and column five the number of thermal pulses calculated. Some low-mass models  $M = 6$ – $3M_{\odot}$  (depending on  $Z$ ) do not undergo enough thermal pulses with dredge-up to obtain an asymptotic value. In these cases we give the largest value found for  $\lambda$ , denoted by  $\lambda_{\text{max}}$  as the value of  $\lambda_{\text{max}}$ . We find no dredge-up for  $Z = 0.02$  mass-loss models of low-mass,  $M_0 \leq 2M_{\odot}$ . Between  $2 < M_0 = M < 3$ , we find  $\lambda_{\text{max}}$  to be smaller for models with mass loss than for those without. There is no appreciable difference in the values of  $\lambda_{\text{max}}$  and  $M_c^{\text{in}}$  for the  $M_0 > 3M_{\odot}$  models with or without mass loss.

Table 3 presents results for  $Z = 0.008$ . For these stars with an LMC composition, the effect of mass loss is seen at lower masses, with masses below  $1.5M_{\odot}$  being the most strongly affected. By  $1.9M_{\odot}$ , mass loss has little effect on the depth of dredge-up, where we find  $\lambda_{\text{max}} = 0.5$  for the model with mass loss compared with  $\lambda_{\text{max}} = 0.6$  for the model without mass loss. Note that for sequences without mass loss we terminated the calculation once an asymptotic value of  $\lambda$  was found. Table 4 presents results for

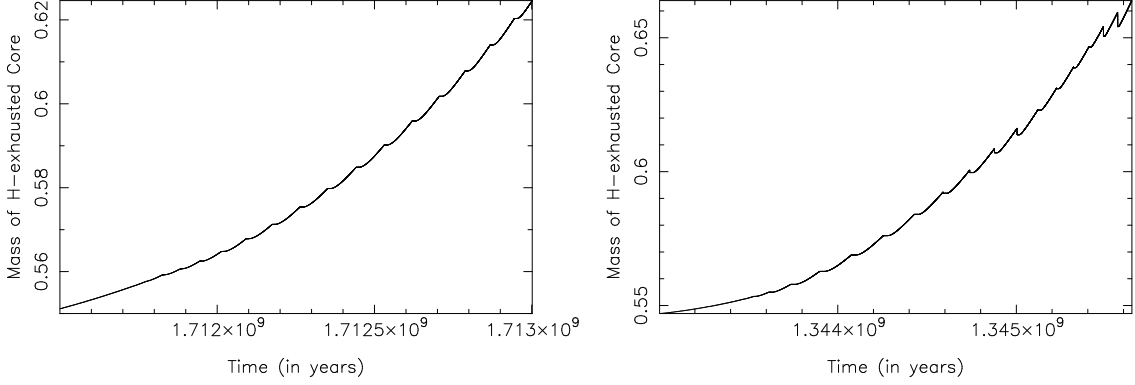


Figure 3: (Left)  $M_c$  against time (years) for a  $M_0 = 1.75 M_\odot$ ,  $Z = 0.02$  model with mass loss. No dredge-up was found. The final  $M_{\text{env}}$  for this model was  $0.0087 M_\odot$ . (Right)  $M_c$  against time (years) for a  $M_0 = 1.75 M_\odot$ ,  $Z = 0.004$  model with mass loss. This model experiences appreciable though erratic dredge-up.  $M_c$  quickly reached  $0.26 M_\odot$ , before being reduced back to zero, then increased right at the end to reach  $0.6 M_\odot$ . This star became a carbon star when  $M_c = 0.615 M_\odot$ ,  $L = 9700 L_\odot$ , and  $M_{\text{bol}} = 5.43$ . The final dredge-up episode takes place with an  $M_{\text{env}} = 0.175 M_\odot$  after the last calculated TP. The final  $M_{\text{env}} = 0.025 M_\odot$ .

$Z = 0.004$ . For this composition mass loss only affects models with  $M < 1.5 M_\odot$  and both the  $1.5$  and  $1.75 M_\odot$  models with mass loss became carbon stars.

Figure 4 shows the  $M_c^1$ ,  $M_c^{\text{min}}$  and  $M_{\text{max}}$  values from Tables 2, 3 and 4 plotted against the initial mass, for all compositions calculated without mass loss. From Tables 2, 3 and 4 we find that  $M_c^1$  and  $M_c^{\text{min}}$  are largely independent of mass loss. The behaviour of  $M_c^1$  in Figure 4 is similar for low-mass stars independent of  $Z$ , with  $M_c^1 \approx 0.55 M_\odot$ . There is a dip in  $M_c^1$  at  $M_0 \approx 2.25 M_\odot$ , corresponding to the transition from degenerate to non-degenerate He-ignition, followed by an increase with increasing initial mass. For models undergoing the SDU ( $M_0 \approx 4 M_\odot$ ) the variation is nearly linear. The value of  $M_c^{\text{min}}$  for low-mass stars ( $M_0 \approx 2.5 M_\odot$ ) decreases somewhat with increasing mass and decreasing  $Z$ , and then shows a similar increase with mass as does  $M_c^1$ . For  $M_0 \approx 4 M_\odot$ ,  $M_c^1$  and  $M_c^{\text{min}}$  are nearly equal, i.e. dredge-up sets in almost immediately after the first pulse.

A comparison with current synthetic calculations is useful. Most calculations have so far assumed a constant value of  $M_c^{\text{min}}$  (Groenewegen & de Jong, 1993), but Marigo (1998a) attempted to improve on this. She assumed dredge-up to occur if, following a pulse, the temperature at the base of the convective envelope reached a specified value  $T_b^{\text{dred}}$ . We compared our  $Z = 0.008$  results for  $M_c^{\text{min}}$  with Figure 3 in Marigo (1998a). For  $M \approx 2.5$ , our values for  $M_c^{\text{min}}$  agree well with her values for  $\log T_b^{\text{dred}} = 6.7$ . Indeed, we find  $\log T_b^{\text{dred}} = 6.7 \pm 0.2$  for all our low-mass models ( $M \approx 2.5 M_\odot$ ) but showing a slight  $Z$  dependence. The  $Z = 0.02$  models required slightly higher temperatures than the lower-metallicity models, with  $\log T_b^{\text{dred}} = 6.8 \pm 0.1$ , whilst the  $Z = 0.008$  and  $Z = 0.004$  models required  $\log T_b^{\text{dred}} = 6.6 \pm 0.1$  for dredge-up. We also note that for deep dredge-up ( $\tau \approx 0.5$ ) the temperature must be higher,  $\log T_b^{\text{dred}} \approx 6.9$ .



Table 2:  $M_c^1$ ,  $m_{ax}$  and  $M_c^{min}$  for  $Z = 0.02$  models without mass loss ( $M = 0$ ) and for models with mass loss ( $M \neq 0$ ). Column one gives the initial mass, with ZAHB mass in parentheses if applicable, column two  $M_c^1$ , column three  $m_{ax}$ , column four  $M_c^{min}$  and column five the number of TPs. Blank entries in the table reflect masses that were not calculated. The meaning of the symbol 'L' is explained in the text.

$M_0$	$M_c^1$		$m_{ax}$		$M_c^{min}$		No. of TPs	
	$M = 0$	$M \neq 0$	$M = 0$	$M \neq 0$	$M = 0$	$M \neq 0$	$M = 0$	$M \neq 0$
1.0 (0.82)		0.542		0.0		{		11
1.25 (1.13)	0.556	0.551	0.0	0.0	{	{	24	10
1.5 (1.41)	0.560	0.556	0.0486 (L)	0.0	0.658	{	24	13
1.75 (1.68)	0.561	0.559	0.223	0.0	0.634	{	28	15
1.9 (1.84)		0.557		0.0		{		18
2.0 (1.96)	0.554	0.551	0.457 (L)	0.00145 (L)	0.632	0.633	27	21
2.25	0.540	0.537	0.709	0.305 (L)	0.624	0.620	37	28
2.5	0.549	0.546	0.746	0.538 (L)	0.625	0.623	36	30
3.0	0.595	0.593	0.790	0.805	0.635	0.630	25	25
3.5	0.662	0.676	0.850	0.880	0.676	0.690	26	22
4.0	0.793	0.792	0.977	0.958	0.799	0.797	22	17
5.0	0.862	0.861	0.955	0.957	0.866	0.864	28	25
6.0	0.915	0.916	0.922	0.953	0.918	0.919	65	40

Table 3: Table of  $M_c^1$ ,  $m_{ax}$  and  $M_c^{min}$  for  $Z = 0.008$ .

$M_0$	$M_c^1$		$m_{ax}$		$M_c^{min}$		No. of TPs	
	$M = 0$	$M \neq 0$	$M = 0$	$M \neq 0$	$M = 0$	$M \neq 0$	$M = 0$	$M \neq 0$
1.0 (0.85)	0.535	0.532	0.0016 (L)	0	0.657	{	22	11
1.25 (1.14)		0.540		0		{		12
1.5 (1.42)	0.550	0.545	0.306	0.0842 (L)	0.624	0.610	21	15
1.75 (1.68)	0.555	0.551	0.532 (L)	0.325 (L)	0.609	0.595	21	15
1.9 (1.85)	0.551	0.549	0.605 (L)	0.500 (L)	0.581	0.594	21	18
2.1	0.540		0.656		0.596		22	
2.25		0.522		0.727 (L)		0.585		27
2.5	0.540	0.541	0.792 (L)	0.805	0.591	0.587	27	28
3.0	0.629	0.629	0.882	0.897	0.639	0.648	20	29
3.5	0.744	0.749	0.957	0.980	0.748	0.756	22	21
4.0	0.830	0.830	0.990	0.970	0.833	0.833	17	24
5.0	0.870	0.870	0.974	0.980	0.871	0.872	27	58
6.0	0.926	0.930	0.932	0.947	0.929	0.933	26	68

Table 4: Table of  $M_c^1$ ,  $M_{c, \text{max}}$  and  $M_c^{\text{min}}$  for  $Z = 0.004$ .

$M_0$	$M_c^1$		$M_{c, \text{max}}$		$M_c^{\text{min}}$		No. of TPs	
	$M_{-} = 0$	$M_{-} \neq 0$	$M_{-} = 0$	$M_{-} \neq 0$	$M_{-} = 0$	$M_{-} \neq 0$	$M_{-} = 0$	$M_{-} \neq 0$
1.0 (0.87)	0.541	0.533	0	0.003 (L)	{	0.611	22	14
1.25 (1.16)		0.541		0.0787 (L)		0.600		14
1.5 (1.43)	0.551	0.549	0.375 (L)	0.325 (L)	0.588	0.601	15	15
1.75 (1.70)	0.558	0.553	0.611 (L)	0.593 (L)	0.589	0.592	16	18
1.9 (1.86)	0.558	0.554	0.669	0.612 (L)	0.589	0.593	18	18
2.1	0.550		0.717 (L)		0.578		16	
2.25	0.537	0.538	0.770	0.767	0.577	0.577	26	26
2.5	0.578	0.577	0.783	0.832	0.607	0.603	15	28
3.0	0.699	0.694	0.963	0.952	0.706	0.702	16	26
3.5	0.804	0.806	0.982	0.998	0.808	0.809	20	23
4.0	0.842	0.842	0.990	0.975	0.845	0.845	20	30
5.0	0.889	0.888	0.970	0.960	0.891	0.890	24	74
6.0	0.962	0.959	0.933	0.940	0.963	0.961	30	95

### 3 Parameterising the Third Dredge-Up

First we will describe the test we made to  $M_c^1$  and then  $M_c^{\text{min}}$  and  $M_{c, \text{max}}$ , followed by a simple prescription to model the variation of  $M_c^1$  with pulse number.

#### 3.1 The Fitting Formula for $M_c^1$

Wagenhuber & Groenewegen (1998) have provided a fitting formula for the core mass at the first thermal pulse,  $M_c^1$  as a function of mass and metallicity (their equation 13). We have compared their Population I test to our results for  $Z = 0.02$ , and found qualitative agreement in the shape of the formula but significant quantitative differences. The same is true for lower metallicities, when we linearly interpolate the coefficients given in Wagenhuber & Groenewegen (1998) for  $Z = 0.008$  and  $Z = 0.004$  and compare the resulting relation to our models.

Here we provide modified coefficients for the fitting formula given by Wagenhuber & Groenewegen (1998), instead of providing a completely new test to  $M_c^1$  as we do for  $M_c^{\text{min}}$  and  $M_{c, \text{max}}$ . We choose to do this for two reasons. Firstly, the shape of the function provided by Wagenhuber & Groenewegen (1998) for  $M_c^1$  (equation 13a-c) is a very good approximation to the shape of the  $M_c^1$ -initial mass relation we find from our models. Secondly, researchers who already use the Wagenhuber & Groenewegen (1998)  $M_c^1$  test for Pop I and II stars in their synthetic evolution codes can easily convert to our test for Pop I, LMC and SMC models. The modified coefficients to the Wagenhuber & Groenewegen (1998) formula can be found in the Appendix. Figure 5 shows the modified tests to  $M_c^1$  plotted against the results from the models without mass loss. Note

that the lines between  $6M_c$  and  $8M_c$  are extrapolations from the fitting functions (valid to  $6M_c$ ) and may not reflect real model behaviour, although one test calculation was made for  $M_c = 6.5$  and  $Z = 0.02$  and did agree with the fits.

### 3.2 The Fitting Formulae for $M_c^{min}$ and $\dot{m}_{max}$

We treat  $\dot{m}_{max}$  as a function of total mass by using a rational polynomial and  $M_c^{min}$  by using a third order polynomial at low masses. At higher masses  $M_c^{min}$  simply follows  $M_c^{1/2}$ . We provide a separate fit for each composition, but interpolation between the coefficients of the polynomials should be possible for arbitrary  $Z$  in the range 0.02 to 0.004.

From Tables 2, 3 and 4 it is clear that if  $M_c^{1/2} > 0.7M_c$ , then  $M_c^{min}$  has a value very close to  $M_c^{1/2}$  (differing by less than  $0.005M_c$ ). Hence it is justified to take  $M_c^{min} = M_c^{1/2}$  in this case. For lower masses generally  $M_c^{min} > M_c^{1/2}$ , and the behaviour of  $M_c^{min}$  is well approximated by a third-order polynomial function. Figure 6 shows the fits made to  $M_c^{min}$  as a function of total mass, for the case without mass loss. The reader is referred to the Appendix for a full description of the polynomial function and the coefficients.

The behaviour of  $\dot{m}_{max}$  is nearly linear at low  $M_c$ , rising steeply with mass until  $M_c \approx 3M_c$  before turning over and flattening out to be almost constant at high mass. This behaviour is shown in Figure 7 for the cases without mass loss. The fits to  $\dot{m}_{max}$  in the figures were made with the function

$$\dot{m}_{max} = \frac{b_1 + b_2 M_c + b_3 M_c^3}{1 + b_4 M_c^3}; \quad (6)$$

where  $b_1, b_2, b_3$ , and  $b_4$  are constants given in the Appendix. We note that as for  $M_c^{1/2}$ , the lines between  $6M_c$  and  $8M_c$  are extrapolations from the fitting functions (valid to  $6M_c$ ) and may not reflect real model behaviour, although one test calculation was made for  $M_c = 6.5$  and  $Z = 0.02$  and did agree with the fits presented here.

### 3.3 Dredge-up Parameter as a function of time

To accurately model the behaviour of the TDU we must include the increase of  $\dot{m}_{max}$  over time. For many of the low-mass models,  $\dot{m}_{max}$  increases slowly, only reaching  $\dot{m}_{max}$  after 8 or more thermal pulses. For the intermediate-mass models,  $\dot{m}_{max}$  approaches  $\dot{m}_{max}$  asymptotically, reaching about  $0.9 \dot{m}_{max}$  in 4 or more thermal pulses but it may not reach  $\dot{m}_{max}$  for many pulses.

To fit the behaviour of  $\dot{m}_{max}$  in the models, we propose a simple method shown in Figure 8. When  $M_c > M_c^{min}$ ,  $\dot{m}_{max}$  starts increasing with pulse number,  $N$ , until asymptotically reaches  $\dot{m}_{max}$  for large enough  $N$ . Since our models gave little information on the decrease of  $\dot{m}_{max}$  with decreasing envelope mass, we suggest  $\dot{m}_{max} = 0$  when  $M_{env} < M_{env,crit}$ , where  $M_{env,crit}$  is some critical value below which dredge-up does not occur. Low-mass models with dredge-up suggest that  $M_{env,crit} \approx 0.2$ .

This behaviour can be modelled with the simple function:

$$\dot{m}_{max}(N) = \dot{m}_{max} (1 - \exp^{-N \tau}); \quad (7)$$

where  $N_r$  is pulse number, measured from the first pulse where the core mass exceeds  $M_c^{min}$ .  $N_r$  is a constant, determining how fast  $\dot{m}$  reaches  $\dot{m}_{max}$ . Due to the nature of the exponential function given by Equation 7, when  $N_r > 8N_r$ , Equation 7 gives a value indistinguishable from  $\dot{m}_{max}$ . Table 5 lists the values of  $N_r$  which give the best fits to the models.

In finding an appropriate value of  $N_r$  for each model, we experimented with different values for each mass. The increase in  $\dot{m}$  observed in some models can be fitted by a range of  $N_r$  values, especially for models that exhibit a lot of scatter in their  $\dot{m}$  values. For example, the  $5M_\odot, Z = 0.02$  model without mass loss is one such case, where we find the range  $4.6 < N_r < 6.6$  gives a reasonable fit to the model as in Figure 8 (left). The depth of dredge-up for the  $5M_\odot, Z = 0.004$  model without mass loss is plotted against two fits from Equation 7 in Figure 8. We note that while the fit with  $N_r = 2$  approximates the model behaviour best, the fit with  $N_r = 4$  is a good fit after 10 or more thermal pulses. We also point out that the  $5M_\odot, Z = 0.004$  model with mass loss experienced 80 TPs, so the first 10 or so pulses will be less important to the final composition of the star than the first 10 pulses of a low-mass model that may only experience 30 or fewer pulses in total before the termination of the AGB phase. For low-mass models with very small values of  $\dot{m}_{max} < 0.1$ , Equation 7 did not result in a good fit regardless of the  $N_r$  value used. We suggest setting  $\dot{m} = \dot{m}_{max}$  when  $M_c > M_c^{min}$  for these low-mass models.

From Table 5 we find a lot of variation in  $N_r$  with mass. Unfortunately, the variation is not systematic and cannot be modelled with a simple function. As we have argued above, the time dependence of  $\dot{m}$  for low-mass stars is quite important as they have few TPs, whilst more massive stars have many TPs so the first pulses are not so influential. Therefore we suggest using a constant  $N_r$  value independent of  $M_0$  for a given  $Z$ , consistent with the low-mass models, e.g.  $N_r = 4$  for  $Z = 0.02$  and  $N_r = 3$  for  $Z = 0.008$  and  $Z = 0.004$ .

Table 5: Table of  $N_r$  values for  $Z = 0.02$ ,  $Z = 0.008$  and  $Z = 0.004$ .

$M_0$	$Z = 0.02$	$Z = 0.008$	$Z = 0.004$
1.5	1	1	2
1.75	3	3	3
1.9	3	2	3
2.25	4	3	3
2.5	4	4	2
3	3.5	4	1
3.5	3	2	1
4	2	2	1
5	5	3	2
6	4	3	3

## 4 Discussion

### 4.1 The Core Mass at the First Pulse

The value of the core mass at the first thermal pulse is perhaps not crucial to synthetic models, because it is the surface composition changes caused by dredge-up that provide constraints on the models. Hence it is  $M_c^{\text{min}}$  that is more important. Nevertheless, comparisons with the CSLF in the Magellanic Clouds indicate that detailed models overestimate  $M_c^{\text{min}}$  and it is useful to know  $M_c^1$  which is in principle the theoretical lower limit for  $M_c^{\text{min}}$ . However,  $M_c^1$  may also be overestimated.

There are few parameterizations of this quantity in the literature. Lattanzio (1989) gave a simple constant value for low mass stars, and Renzini & Voli (1981) gave a fit for more massive models. These were used by Groenewegen & de Jong (1993). A more detailed fit was given by Wagenhuber & Groenewegen (1998), which was used by Marigo (2001). This latter fit reproduces the shape very well. We have simply modified the coefficients as described in Section 3.1 to provide a much better fit to the current results.

### 4.2 Dredge-up: $M_c^{\text{min}}$ and $\tau_{\text{max}}$

Most synthetic calculations use constant  $M_c^{\text{min}}$  and constant  $\tau$ . Groenewegen & de Jong (1993) used the constant values given by Lattanzio (1989) for  $M_c^{\text{min}}$ , and then adjusted  $\tau$  to try to fit the CSLF of the Magellanic Clouds. They found that  $M_c^{\text{min}}$  must also be decreased from the theoretical value, and they settled on  $M_c^{\text{min}} = 0.58$  and  $\tau = 0.75$  to fit the observations. A similar procedure was followed by Marigo et al. (1996) and they found  $M_c^{\text{min}} = 0.58$  and  $\tau = 0.65$ . Note that Marigo (2001) now uses a more sophisticated algorithm for determining the onset of dredge-up, as discussed in section 2.4.

The parameterizations we have given here should be a significant improvement to the constant values used for most synthetic studies. In the discussion below we will compare our results with other detailed evolutionary calculations.

From Figure 4 we find  $\tau_{\text{max}}$  to increase with decreasing  $Z$  for a given mass, so we find low-mass models ( $M_0 \approx 2M_\odot$ ;  $Z = 0.008; 0.004$  with mass loss) can become carbon stars with  $\tau_{\text{max}}$  as high as 0.6 for the  $1.75M_\odot$ ;  $Z = 0.004$  model. This effect is not so noticeable for higher mass stars ( $M_0 \approx 4M_\odot$ ), where dredge-up quickly deepens with pulse number, and  $\tau_{\text{max}} \approx 0.9$  for all compositions.

In comparison, Vassiliadis (1992), who used a different version of the Mount Stromboli stellar evolution code (Wood & Faulkner 1986, 1987) and older opacities (Huebner et al., 1977), only found dredge-up for  $M_0 > 2.5M_\odot$  for LMC abundances and for  $M_0 > 2.0M_\odot$  for SMC abundances. Clearly, the larger OPAL opacities we use (Frost 1997) and the improved modelling of the TDU by Frost & Lattanzio (1996) make a considerable difference.

Straniero et al. (1997), using the OPAL opacities find  $\tau_{\text{max}} \approx 0.3$  for a solar composition  $1.5M_\odot$  model without mass loss. On the other hand, we find  $\tau_{\text{max}} \approx 0.05$ , substantially lower for the same mass and composition. This is probably due to

the difference in mixing-length parameter: we used 1.75 and Straniero et al used the higher value of 2.2. A test calculation with a mixing-length parameter of 2.0 yielded  $\tau_{\text{max}} = 0.2$ . We find deeper dredge-up than Straniero et al for the  $3M_{\odot}; Z = 0.02$  model (without mass loss) with  $\tau_{\text{max}} = 0.75$  where they find  $\tau_{\text{max}} = 0.46$ . These discrepancies must also be related to the numerical differences between the codes (Frost & Lattanzio 1996; Lugaro 2001).

We find very similar values of  $\tau$  to Pols & Tout (2001) for the  $5M_{\odot}, Z = 0.02$  model. These authors use a fully implicit method to solve the equations of stellar structure and convective mixing, and they find  $\tau$  to increase to 1.0 in only six TPs while our models reach  $\tau = 0.95$  much more slowly (see Figure 6).

Herwig (2000) includes diffusive convective overshoot during all evolutionary stages and on all convective boundaries on two solar composition models of intermediate mass. Without overshoot, no dredge-up is found for the  $3M_{\odot}$  model. With overshoot, efficient dredge-up is found for both the 3 and  $4M_{\odot}$  models, where  $\tau < 1$  for the  $3M_{\odot}$  model and  $\tau > 1$  for the  $4M_{\odot}$  model, which has the effect of decreasing the mass of the H-exhausted core over time. Clearly, the inclusion of convective overshoot can substantially increase the amount of material dredged up from the intershell to the surface. Langer et al. (1999) using a hydrodynamic stellar evolution code, model the effects of rotation on the structure and mixing of intermediate mass stars, also find some dredge-up in a  $3M_{\odot}$  model of roughly solar composition.

### 4.3 The Carbon Star Luminosity Function

The most common observation used to test the models is the reproduction of observed CSLFs. We note that mass loss has the largest effect on the  $Z = 0.02$  models and we do not find any dredge-up for  $M < 2M_{\odot}$ . It seems likely that our  $Z = 0.02$  models with mass loss cannot reproduce the low-mass end of the galactic carbon star distribution, with progenitor masses in the range  $1 < M < 3M_{\odot}$  (Wallerstein & Knapp, 1998) as we find no dredge-up for models with mass-loss with  $M_0 < 2.0M_{\odot}$ . The lowest mass solar composition model to become a carbon star is the  $3M_{\odot}; Z = 0.02$  model, which has  $C/O > 1$  after 22 thermal pulses. We do note, however, that the galactic CSLF is very uncertain.

However, for LM C and SM C compositions, the CSLF is very well known (see discussion in Groenewegen & de Jong 1993). It is a long standing problem that detailed evolutionary models fail to match the observed CSLFs in the LM C and SM C (Iben 1981). Although many of our models with LM C and SM C compositions show enough dredge-up to turn them into carbon stars we expect that they will not fit the low luminosity end of the CSLF, because we find small values of  $\tau$  for  $M < 1.5M_{\odot}$ , less than the value found from synthetic calculations of  $\tau = 0.5$  as the required value to fit the CSLF. Also, we find larger  $M_c^{\text{min}}$  values for our LM C and SM C low-mass models than the  $0.58M_{\odot}$  found from synthetic AGB calculations (Groenewegen & de Jong, 1993; Marigo 1996, 1998a,b).

Within the context of synthetic models one usually modifies the dredge-up law to ensure that agreement is reached. This usually means decreasing  $M_c^{\text{min}}$  and increasing

, although this has previously been done crudely by altering constant values for all masses (possibly with a composition dependence)<sup>3</sup>. The models presented here show the variation with mass and composition of all dredge-up parameters. This has not been available previously. Although modifications may be required, perhaps caused by our neglect of overshoot (Herwig, 1997, 2000) or rotation (Langer et al., 1999), we expect the dependence on mass and composition to be retained.

## 5 Conclusions

We have presented extensive evolutionary calculations covering a wide range of masses and compositions, from the ZAMS to near the end of the AGB. Later papers will investigate nucleosynthesis and stellar yields, but in this paper we concerned ourselves with determining the dredge-up law operating in the detailed models. We have given parameterised fitting formulae suitable for synthetic AGB calculations. As they stand, we expect that these will not fit the observed CSLFs in the LMC and SMC, a long-standing problem. Some adjustments may be necessary, but must be consistent with the dependence on mass and composition as presented here. This may constrain the adjustments and lead to a better understanding of where the detailed models can be improved.

## Appendix

### Coefficients for the fit to $M_c^1$

The equations used by Wagenhuber & Groenewegen (1998) to fit  $M_c^1$  are

$$M_c^1 = (p_1(M_0 - p_2)^2 + p_3)f + (p_4M_0 + p_5)(1 - f); \quad (8)$$

$$f = \frac{1}{1 + e^{\frac{M_0 - p_6}{p_7}}}; \quad (9)$$

Equations 8 and 9 are almost constant for stars with  $M_0 < 2.5M_\odot$  and almost linear for stars that experience the second dredge-up (for masses greater than about  $4M_\odot$ ). The constant coefficients,  $p_1$  through to  $p_7$  that best fit our model results, are given in Table 6.

### Coefficients for the fits to $M_c^{min}$ and $M_c^{max}$

Let  $M_{sdu}$  be the minimum mass, at a given composition, which experiences the second dredge-up. Hence from our models  $M_{sdu} = 4M_\odot$  for  $Z = 0.02$ ,  $3.8M_\odot$  for  $Z = 0.008$  and  $3.5M_\odot$  for  $Z = 0.004$ . For masses  $M_0 < M_{sdu}$ , our results for  $M_c^{min}$  are fitted to a cubic polynomial,

$$M_c^{min} = a_1 + a_2M_0 + a_3M_0^2 + a_4M_0^3 \quad (10)$$

<sup>3</sup>Note that Marigo (1998a) adjusted her algorithm via a reduction of  $T_p^{dred}$  to 6.4 from the 6.7 found in detailed models.

Table 6: Coefficients for Equations 8 and 9:  $p_1, p_2, p_3, p_4, p_5, p_6$  and  $p_7$ .

Z	$p_1$	$p_2$	$p_3$	$p_4$	$p_5$	$p_6$	$p_7$
0.02	0.038515	1.41379	0.555145	0.039781	0.675144	3.18432	0.368777
0.008	0.057689	1.42199	0.548143	0.045534	0.652767	2.90693	0.287441
0.004	0.040538	1.54656	0.550076	0.054539	0.625886	2.78478	0.227620

where  $a_1, a_2, a_3$  and  $a_4$  are constants that depend on  $Z$  and are given in Table 7 and  $M_0$  is the initial mass of the star (in solar units).

For cases where  $M_0 \leq M_{\text{sdm}} = 0.5M_\odot$  we find that  $M_c^{\text{min}} > 0.7M_\odot$ , and we can set  $M_c^{\text{min}} = M_c^1$  consistent with our model results. Since Eq. 10 diverges for large masses, in practice we recommend calculating  $M_c^{\text{min}}$  by the following procedure:

$$M_c^{\text{min}} = \max(M_c^1; \min(0.7M_\odot; M_c^{\text{min}})) \quad (11)$$

where  $M_c^{\text{min}}$  is given by Eq. 10. This ensures that always  $M_c^{\text{min}} > M_c^1$  as required, while  $M_c^{\text{min}} = M_c^1$  if  $M_c^1 > 0.7M_\odot$ .

Table 7:  $a_1, a_2, a_3$  and  $a_4$  for Equation 10.

Z	$M_c^{\text{min}}$			
	$a_1$	$a_2$	$a_3$	$a_4$
0.02	0.732759	-0.0202898	-0.0385818	0.0115593
0.008	0.672660	0.0657372	-0.1080931	0.0274832
0.004	0.516045	0.2411016	-0.1938891	0.0446382

We fit  $t_{\text{max}}$  with a rational polynomial of the type given in Equation 6. The constants,  $b_1, b_2, b_3$  and  $b_4$  for  $Z = 0.02, Z = 0.008$  and  $Z = 0.004$  are given in Table 8. For  $Z = 0.02$ , we only fit  $t_{\text{max}}$  and  $M_c^{\text{min}}$  down to  $1.5M_\odot$  and as a consequence the  $t_{\text{max}}$  goes negative for masses below this. For  $Z = 0.008$  and  $Z = 0.004$ , we fit  $t_{\text{max}}$  and  $M_c^{\text{min}}$  down to  $1M_\odot$ . Therefore, if Equation 6 yields a negative value  $t_{\text{max}}$  should be set to zero.

Table 8:  $b_1, b_2, b_3$  &  $b_4$  for Equation 6 for  $t_{\text{max}}$

Z	$t_{\text{max}}$			
	$b_1$	$b_2$	$b_3$	$b_4$
0.02	-1.17696	0.76262	0.026028	0.041019
0.008	-0.609465	0.55430	0.056878	0.069227
0.004	-0.764199	0.70859	0.058833	0.075921

It is possible to linearly interpolate between the coefficients in  $Z$  to find fits for intermediate metallicities. This may not reflect real model behaviour but the functions



are well behaved. Note that interpolating between the coefficients of Equation 6 in the range  $0.02 < Z < 0.008$  will result in negative values of  $\dot{m}_{\text{ax}}$  between  $1.6 M_{\odot} (M_{\odot})$  6 1.5. Again we suggest setting  $\dot{m}_{\text{ax}} = 0$  when this happens.

## Acknowledgments

I would like to acknowledge the assistance of a Monash Graduate Scholarship for support and the Victorian Partnership for Advanced Computing for computational time and support. We also thank the anonymous referees for helping to improve the clarity of the paper.

## References

- Boothroyd, A. I. & Sackmann, I. -J., 1988, *ApJ*, 328, 671
- Busso, M., Gallino, R. & Wasserburg, G., 1999, *ARA&A*, 37, 329
- Frost, C. A., 1997, Ph.D. Thesis, Monash University
- Frost, C. A. & Lattanzio, J. C., 1995, in *Stellar Evolution: What Should Be Done?*
- Frost, C. A. & Lattanzio, J. C., 1996, *ApJ*, 344, L25
- Groenewegen, M. A. T. & de Jong, T., 1993, *A&A*, 267, 410
- Herwig, F., 2000, *A&A*, 360, 952
- Herwig, F., Blocker, T., Schonbemer, D., El Eid, M., 1997, *A&A*, 324, L81
- Huebner, W. F., Merts, A. L., Magee, N. H. Jr. & Argo, M. F., 1977, *Astrophysical Opacity Library*, Los Alamos Scientific Laboratory, LA-6760-M
- Hurley, J. R., Tout, C. A., Pols, O. R., 2002, *MNRAS*, 329, 897
- Iben Jr., I., 1981, *ApJ*, 246, 278
- Iben Jr., I., 1991, ed. G. Michaud, A. V. Tutukov, in *Evolution of Stars: The Photospheric Abundance Connection*, (Dordrecht, Kluwer Academic Publishers), 257
- Iglesias, C. A. & Rogers, F. J., 1996, *ApJ*, 464, 943
- Langer N., Heger A., Wellstein S., Herwig F., 1999, *A&A*, 346, L37
- Lugaro, M. A., 2001, Ph.D. Thesis, Monash University
- Marigo, P., Bressan, A. & Chiosi, C., 1996, *A&A*, 313, 545
- Marigo, P., 1998a, in *Asymptotic Giant Branch Stars*, ed. T. Le Bertre, A. Lebre, C. Wealkens, (Astronomical Society of the Pacific), 53
- Marigo, P., Bressan, A. & Chiosi, C., 1998b, *A&A*, 331, 564
- Marigo, P., 2001, *A&A*, 370, 194
- Mowlavi, N., 1999, *A&A*, 344, 617
- Pols, O. R., Tout, C. A., 2001, in *Salting the Early Soup: Trace Nuclei from Stars to the Solar System*, ed. M. Busso & R. Gallino, *Mem. S.A.It.*, v72 No. 2, in press.
- Straniero, O., Chie, A., Limongi, M., Busso, M., Gallino, R. & Randini, C., 1997, *ApJ*, 478, 332
- Reimers, D., 1975, in *Problems in Stellar Atmospheres and Envelopes*, ed. B. Baschek, W. H. Kegel, G. Traving, (New York: Springer-Verlag), 229
- Wagenhuber, J. & Groenewegen, M. A. T., 1998, *A&A*, 340, 183

W allerstein, G . & Knapp, G . R . , 1998, ARA & A , 36, 369  
W ood, P . R . & Faulkner, D . J, 1986, ApJ, 307, 659  
W ood, P . R . & Faulkner, D . J, 1987, PASA , 7, 75  
W ood, P . R . & Zarro, D . M . , 1981, ApJ, 248, 311  
van den Hoek, L . B . & Groenewegen, M . A . T , 1997, A & A SS, 123, 305  
Vassiliadis, E . , 1992, Ph D . Thesis, Australian National University  
Vassiliadis, E . & W ood, P . R . , 1993, ApJ, 413, 641

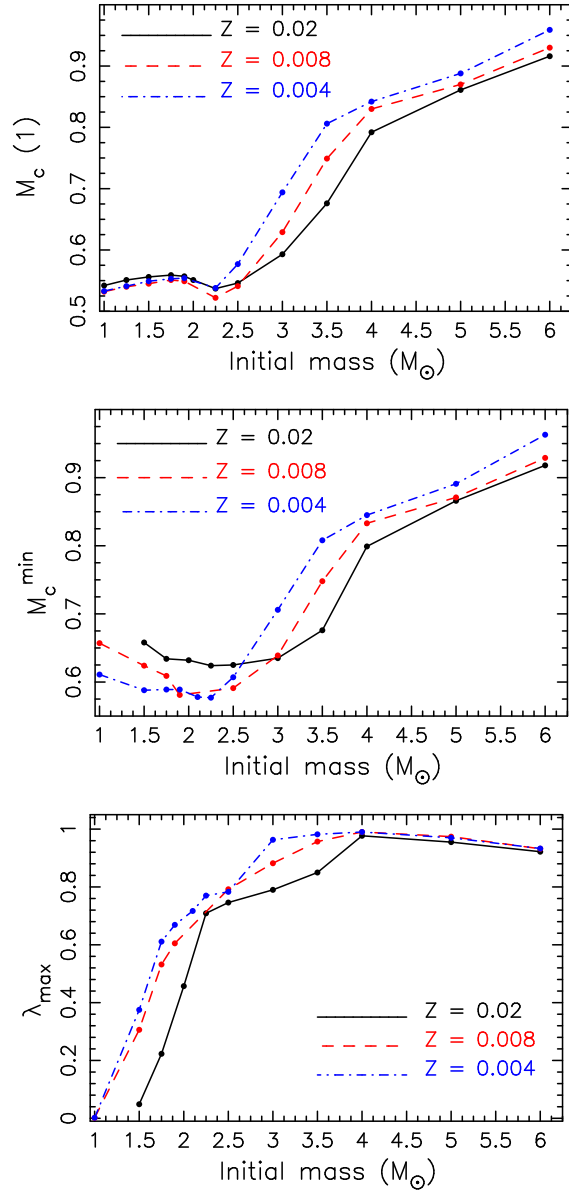


Figure 4: The  $M_c^1$ ,  $M_c^{\min}$  and  $\lambda_{\max}$  plotted against initial mass for the  $Z = 0.02$ ,  $Z = 0.008$  and  $Z = 0.004$  models without mass loss. In each panel, the blue solid line refers to the  $Z = 0.02$  models, the black dashed line to the  $Z = 0.008$  models and the red dash-dotted line to the  $Z = 0.004$  models.

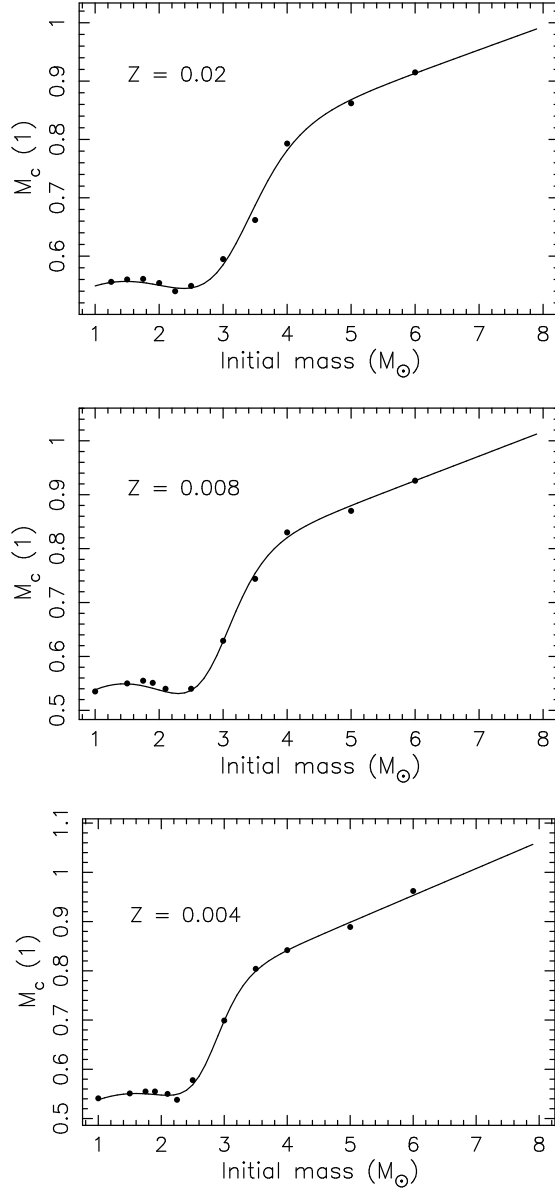


Figure 5: The  $M_c$  to  $M_c^1$  using the Wagenhuber & Groenewegen (1998) with modified coefficients (solid line) plotted with model results for the  $Z = 0.02$ ,  $Z = 0.008$  and  $Z = 0.004$  models without mass loss.

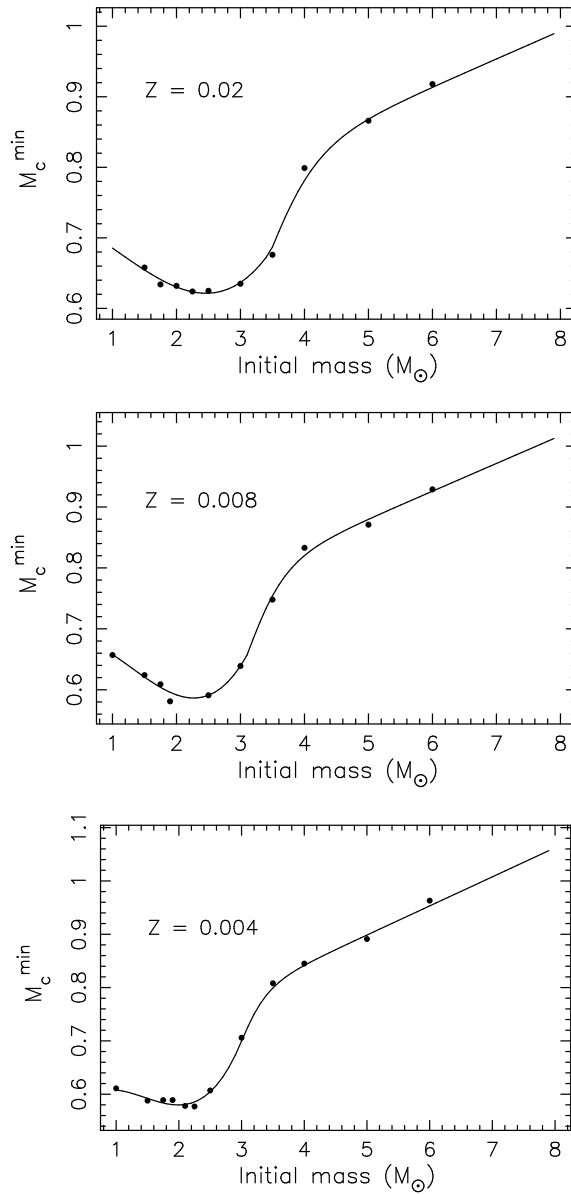


Figure 6: The  $t$  to  $M_c^{\min}$  (solid line) for  $Z = 0.02$ ,  $Z = 0.008$  and  $Z = 0.004$ , plotted with results (points) from the models without mass loss.

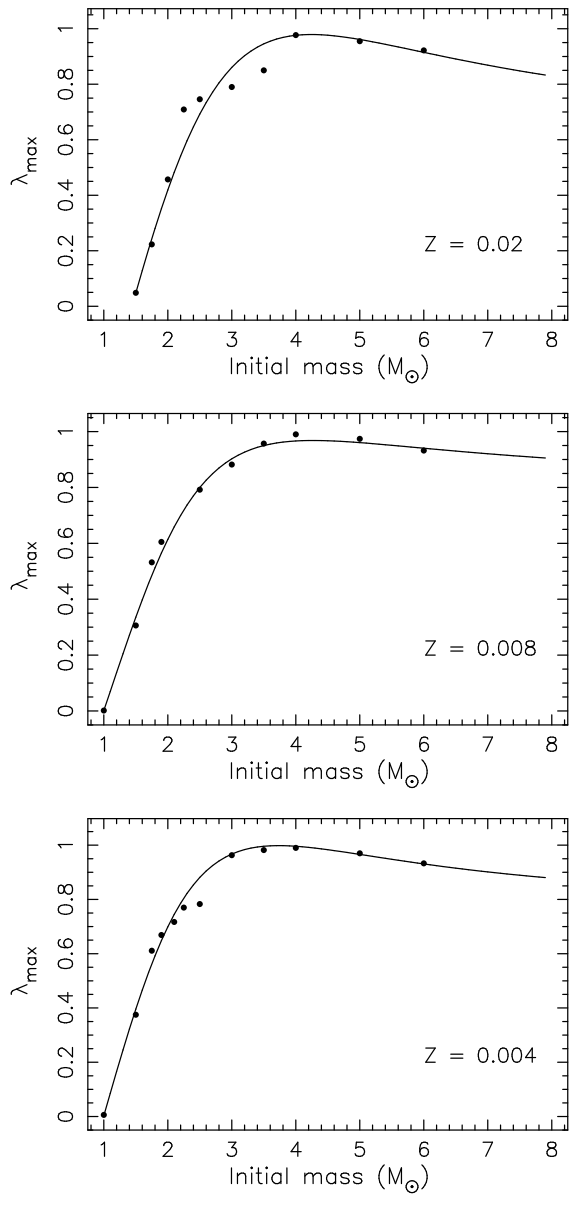


Figure 7: The  $t$  to  $m_{\max}$  (solid line) for  $Z = 0.02$ ,  $Z = 0.008$  and  $Z = 0.004$ , plotted with results (points) from the models without mass loss.

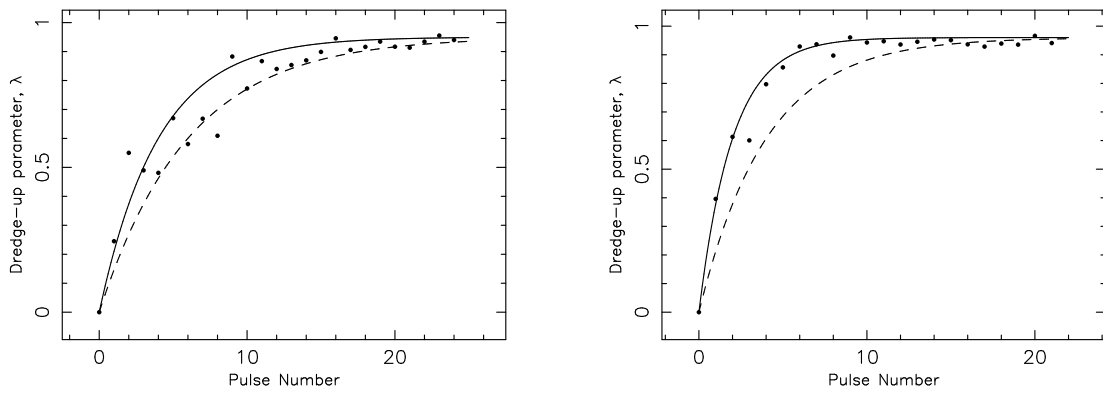


Figure 8: (Left) Fit to  $\lambda$  from Equation 7 with  $N_r = 4$  (solid line) and  $N_r = 6$  (dashed line) for the 5M,  $Z = 0.02$  sequence without mass loss (points). We found the best fit to be  $N_r = 5$ . (Right) Fit to  $\lambda$  from Equation 7 with  $N_r = 2$  (solid line) and  $N_r = 4$  (dashed line) for the 5M,  $Z = 0.004$  sequence without mass loss.